NINETEENTH EUROPEAN ROTORCRAFT FORUM

Paper No: D15

AN INITIAL EVALUATION OF BLADE DYNAMICS OF A STOPPED/FLIPPED ROTOR WITH FLAP CONTROLS

Y. K. YILLIKCI
Istanbul Technical University
Faculty of Aeronautics and Astronautics
80626 Maslak, Istanbul, TURKIYE

S. HANAGUD
Georgia Institute of Technology
CERWAT and School of Aerospace Engineering
Atlanta GA 30332 USA

September 14-16, 1993
CERNOBBIO (Como)
ITALY

ASSOCIAZIONE INDUSTRIE AEROSPAZIALI
ASSOCIAZIONE ITALIANA DI AERONAUTICA
ED ASTRONAUTICA

AN INITIAL EVALUATION OF BLADE DYNAMICS OF A STOPPED/FLIPPED ROTOR WITH FLAP CONTROLS

Y. K. Yillikçi *
Istanbul Technical University, Turkiye

S. Hanagud †
Georgia Institute of Technology USA

Abstract

A conditionally stable explicit finite difference scheme is used to numerically integrate the nonlinear partial differential equations of motion in space and time to obtain the aeroelastic transient response of a hingeless rotor blade with trailing edge flap controls. New aerodynamic environment due to flap control is formulated based on Theodorsen's unsteady oscillating airfoil aerodynamics representation including unsteady trailing edge flap motions. A simplified trim procedure is coupled with the nonlinear P.D.E. solver to simulate elastic blade tip deflections during rotor stopping transition.

LIST OF SYMBOLS

C_W	helicopter weight coeff.
$C_{L_{can}}$	canard lift coeff. $\frac{L_{can}}{\rho\pi R^4\omega^2}$
$C_{T_{MR}}$	main rotor trust coeff. $\frac{T_{MR}}{\rho\pi R^4\omega^2}$
$\bar{G}\bar{J}$	nondim. torsional stiffness, $\frac{GJ}{m_{ref}\Omega^2R^4}$
L_v, L_w	lift in v and w directions, fl^{-1}
M_ϕ	aerodynamic moment per unit length, f
u, v, w	elastic displacements in x,y,z directions, l
U_P, U_T	velocity components of airfoil, in lagwise and flapwise directions, lt^{-1}
γ	Lock number
λ_0	rotor induced uniform inflow,
Λ_1, Λ_2	nondimensional, $\frac{EI_{y'}}{m_{ref}\Omega^2R^4}$, $\frac{EI_{z'}}{m_{ref}\Omega^2R^4}$
$\Lambda_0, \Lambda_{1S}, \Lambda_{1c}$	collective and cyclic flap control inputs, rad
μ	nondim. forward speed, $\frac{V}{\Omega^2R}$
σ	solidity, $\frac{bc}{\pi R}$
ϕ	rotation about elastic axis including bending and torsion,rad
ψ	nondim. time or azimuth angle, $\psi = \Omega t$, rad Ω rotor speed, $rad\ t^{-1}$

INTRODUCTION

Flap Controlled Rotor Blade Concept

The use of swash-plate systems for applying collective and cyclic pitch change has been the primary element of helicopter controls since the earlier phases of its development. Almost today's all rotorcrafts involve swash-plate system as the main control device for adjusting the blade pitch angle in order to balance aerodynamic lift and moment distribution. The application of trailing edge flaps to manipulate rotor blade lift variation was first introduced by Charles KAMAN, a distinguished helicopter pionner, and the concept called *servo-flap* was successfully used in several Kaman helicopters.

With the development of advanced sensors, actuators, command-control systems and demand for new technologies for blade control mechanisms; flap and servo-flap control concepts have been started to be analyzed with new objectives. Possible applications of flap controlled rotor systems for Army's

*Asst. Prof, Faculty of Aeronautics and Astronautics, Formerly UAV Project Coordinator at Undersecretariat For Defense Industries

†Professor, CERWAT and School of Aerospace Engineering,

Presented at Nineteenth European Rotorcraft Forum, 14-16 September 1993, Cernobbio, Italy.

High Maneuverability/Agility Rotor Control System (HIMARCS) and conceptual designs of Kaman, Bell and MDHC helicopters have been evaluated detailly in references [1, 2, 3] respectively.

Additional control parameters introduced by flap controls expected to give designers additional flexibilities in tailoring aeroelastic and aerodynamic characteristics of next century's rotor blades. With multi-input flap controls located at outboard section of the blade more efficient blade controls can be achieved with smaller control surfaces. With these expectations complete replacement of standart pitch control with flap control particularly for a 700 lb micro-helicopter configuration is first evaluated by reference [4]. Periodic response of an elastic rotor blade with flap control has been analyzed by reference [5] and tip deflections of the flap controlled elastic blade have been compared with the pitch controlled identical blade. Response characteristics of both control cases are found to be almost identical except for the elastic twist which was obtained higher for the flap controlled blade. Major features of the standart pitch control and the proposed flap control can be outlined as follows

- CONTROL INPUT
  Standart pitch control is applied by a fully mechanical swashplate and it is limited up to the first harmonics as,
  $$\theta = \theta_0 + \theta_{1s} \sin\psi + \theta_{1c} \cos\psi$$
  On the other hand flap control can be applied as a contoured time dependent surface motion at the trailing edge of the blade. For initial evaluation studies and for comparision simplicity flap control is formulated at this stage as;
  $$\Lambda = \Lambda_0 + \Lambda_{1s} \sin\psi + \Lambda_{1c} \cos\psi$$
  Flap control is expected to be applied by electro-mechanical, piezo-ceramic based actuators with the use highly flexible flap surfaces.

- AEROYNAMICS
  Aerodynamically, a periodic trailing edge flap motions will be less disturbing for the flow field around the rotor blade compared to a pitching airfoil. As known pitching and flapping blade tips causes vortices and dynamic stall which are highly undesirable. For the flap controlled case, contoured flap motions can reduce these flow disturbances and a non-pitching blade tip is expected to face much less dynamic stall conditions as compared with the pitching airfoil.

- HIGH HARMONIC AND INDIVIDUAL BLADE CONTROLS
  Standart pitch controlled rotors require additional actuators for each blade for controls with higher harmonics. Flap controls can be applied in principle at desired frequencies independent from the blade rotation frequencies. Utilized with a series of sensors and related logical systems high bandwidth active controls can practically achived which are essential for individual blade control.

Stopped/Flipped Rotor Concept

Tipjet VTOL Unmanned Air Vehicle (UAV) concept have been introduced as an alternative VTOL UAV configuration and recently a series design and development studies have been performed for a 1200 lb shipboard tipjet VTOL UAV system at David Taylor Naval Research and Development Center (DTNRD) which utilizes circulation control for lift augmentation during rotary wing mode [6]. Tipjet general characteristics are outlined as;

- High aspect ratio monoplane wing which becomes 2-bladed tipjet helicopter rotor for shipboard launch/recovery and as by product an oblique wing capability for high speed dash.
- Single turbofan engine provides; fixed wing propulsion and tipjet rotor drive,
- Circulation controlled (CC) airfoil provides; good loiter performance and helicopter controllability with no wing/rotor articulation,
- Costs of VTOL UAV are; i) fan diffuser/plenum, wing/rotor breake, variable tip and propulsion nozzles, ii) high fan pressure ratio which slightly increases specific fuel consumption.

Complete elimination of the swashplate mechanism along with the possibility of intelligent/ smart rotor blade control features brought an alternative approach for the stopped rotor UAV concept and a stopped/flipped rotor helicopter with flap controls was introduced by Reference [7]. The basic idea behind this stopped rotor concept can be outlined as follows. Proposed air vehicle is supposed to have a lifting surface with high aspect ratio and it will perform as a helicopter rotor during take-off, low altitude flight, low speed maneuvers at initial climb mode. At proper altitude and forward

speed, the rotor will be gradually stopped and one of the blades will be flipped 180 degrees around its spanwise axis in order to replace the leading edge with the trailing edge. During this transition, forward propulsion will be also replaced by a pusher propeller and the vehicle will continue to fly as a fixed wing after this conversion. General configuration of the proposed stopped/flipped rotor and the concept of flap control are shown in Figure 1.

Basic features of the proposed stopped/flipped rotor configuration can be outlined as;

- Complete helicopter VTOL flight and maneuver capabilities,
- High aspect ratio, oblique-wing and canard configuration for high dash speeds,
- Lift augmentation with the use of canard and tail wing surfaces during rotor stop transition and forward flight modes,
- Flap controlled blade/wing provides wide bandwith control for basic, high harmonic and individual blade control for rotary wing and excellent fixed wing flap controls,
- Use of installed power in both flight modes; helicopter vertical take-off and high speed forward flight.

A practical application of tipjet VTOL UAV will first require the development of a highly complex air circulation control system which includes fan diffusers, plenums and a series of variable tip and propulsion nozzles. On the other hand realization of the stopped/flipped rotor mechanism requires a series of research and engineering studies for first understanding the new control mechanism and secondly to implement it to practical applications. Research and design challenges required for the development of the stopped/flipped rotor can be outlined as;

- Dynamic modeling and analysis of rotor blade during rotor rpm drop and instant braking along with the aeromechanical stability of entire vehicle during this transition,
- Rotor aerodynamics during rotor flipping must be well defined.
- New control laws to utilize multi-input/multi-output control mechanisms; rotor control input higher harmonics ($\Lambda_{2s}, \Lambda_{2c}, ...\Lambda_{nc}$) and canard wing lift control inputs ($\delta_{can_l}, \delta_{can_r}, ..etc$) must be included vehicle flight control modelling.

FORMULATION

Aeroelastic modelling of flap controlled rotor blade is consisted of three major steps. First step of the problem is the formulation and calculation of flap control trim settings for the choosen helicopter configuration. The second step of is the formulation of new aerodynamic environment around the rotor blade. The new set of rotor blade nonlinear partial differential equations are solved numerically as the third step.

Trim Formulations

Trim setting of the rotor blade configuration where all conventional collective and cyclic pitch controls are replaced with cyclic trailing edge flap controls are calculated by a two step procedure. At the first step, trim settings for the cyclic pitch case for the choosen helicopter configuration are calculated by the use of standart trim equations given in Reference [8]. As the second step, rigid blade flapping which is expressed as,

$$\beta = \beta_0 + \beta_{1s} \sin\psi + \beta_{1c} \cos\psi \tag{1}$$

and control inputs of the flap control represented up to its first harmonics as;

$$\Lambda = \Lambda_0 + r\ \Lambda_{TW} + \Lambda_{1s} \sin\psi + \Lambda_{1c} \cos\psi \tag{2}$$

where Λ_{tw} 's build-in twist flap setting. Based on these representations, trim setting are calculated as described in the next section.

Since the overall configuration and the rotor blade planeform are kept identical both for pitch control and flap control cases; trim results as, $\beta_{1s,}, \beta_{1c}, \alpha_v, \phi_v, C_{T_{mr}}, C_H, C_Y, C_p$ of the pitch controlled configuration are assumed to be identical for the flap control case. Trust generated with the rotor blade with flap control is formulated based on the sectional lift is written as,

$$\frac{F_Z}{\sigma a} = \frac{1}{2}\left[U_T^2\theta_{ri} - U_P U_T\right] + \left[\frac{c}{4a}(f_2 - f_3)U\ \overset{*}{\Lambda} - \frac{c^2}{8a} f_4\ \overset{**}{\Lambda} + \frac{1}{a} f_1 U^2 \Lambda\right] \tag{3}$$

where f_1, f_2, f_3 and f_4 are parameters due to the flap geometry and are given in reference [5], $(\overset{*}{\ }) = \frac{\partial}{\partial \psi}$ and $(\overset{**}{\ }) = \frac{\partial^2}{\partial \psi^2}$. In standart trim formulations θ_{ri} is replaced by θ control input which is conventionally expressed as

$$\theta = \theta_0 + r\ \theta_{TW} + \theta_{1s} \sin\psi + \theta_{1c} \cos\psi \tag{4}$$

The second term of equation 3 is representing the sectional lift due to the cyclic trailing edge flap motion and derived based on Theodorsen's two-dimensional unsteady aerodynamics of oscillating airfoils and details of the aerodynamic formulation are given in the next section. By the use of equation 3 mean of the rotor trust is written as,

$$\begin{aligned} \frac{C_{T_0}}{\sigma a} &= \frac{1}{2}\left(C_{12} + C_{10}\frac{\mu^2}{2}\right)\theta_{ri} - \frac{1}{2}C_{11}\lambda - d_{1k0}\frac{\mu}{2}\Lambda_{1c} + \left(d_{3k2} + d_{3k0}\frac{\mu^2}{2}\right)\Lambda_0 \\ &+ \left(d_{3k3} + d_{3k1}\frac{\mu^2}{2}\right)\Lambda_{TW} + d_{3k1}\mu\Lambda_{1s} \end{aligned} \tag{5}$$

Parameters $C_{10}, C_{11}, ..., d_{3k3}$ are related with blade chord and flap geometries and are given in reference [5]. Additional to the average trust formulation, rotor blade rigid flapping dynamics for variable blade geometry is needed to be formulated. Flapping dynamics of rigid rotors without flapping hinge offset is given in reference [8] as,

$$\overset{**}{\beta} + \beta = \frac{1}{2}\frac{\rho c a R^4}{I_b}\int_0^1 r F_Z dr \tag{6}$$

where blade flapping β is represented up to its first harmonics and equation 6 gives three additional equations for the trim calculations. Equations 5 and 6 are rearranged in matrix form as

$$\mathbf{A}_g \mathbf{x}_g = \mathbf{q}_g \tag{7}$$

where,

$$\mathbf{A}_g = \begin{bmatrix} \frac{1}{\gamma} & -(d_{3k3} + d_{3k1}\frac{\mu^2}{2}) & -d_{3k2}\mu & d_{1k1}\frac{\mu}{2} \\ 0 & -2d_{3k2}\mu & -d_{2k1} - (d_{3k3} + d_{3k1}\frac{3}{4}\mu^2) & d_{1k2} \\ \frac{1}{2}C_{12}\mu & 0 & -d_{1k2} & -d_{2k1} - (d_{3k3} + d_{3k1}\frac{\mu^2}{4}) \\ 0 & (d_{3k2} + d_{3k0}\frac{\mu^2}{2}) & d_{3k1}\mu & -d_{1k0}\frac{\mu}{2} \end{bmatrix}$$

$$\mathbf{q}_g = \begin{Bmatrix} -\frac{1}{2}(C_{13} + C_{11}\frac{\mu^2}{2})\theta_{ri} - \frac{1}{2}C_{12}\lambda + (d_{3k4} + d_{3k2}\frac{\mu^2}{2})\theta_{tw} \\ C_{12}\mu\theta_{ri} + \frac{1}{2}(C_{13} - C_{11}\frac{\mu^2}{4})\beta_{1c} - \frac{\mu\lambda}{2}C_{11} + 2d_{3k3}\mu\theta_{tw} \\ -\frac{1}{2}(C_{13} + C_{11}\frac{\mu^2}{4})\beta_{1s} \\ -\frac{1}{2}(C_{12} + C_{10}\frac{\mu^2}{2})\theta_{ri} + \frac{1}{2}C_{11}\lambda - (d_{3k3} + d_{3k1}\frac{\mu^2}{2})\Lambda_{tw} + \frac{C_{T_{m.r}}}{\sigma a} \end{Bmatrix}$$

and vector $\mathbf{x}_g = \{\beta_0^\Lambda, \Lambda_0, \Lambda_{1s}, \Lambda_{1c}\}^T$ represents the trim settings to be calculated for the flap control case. In formulation given by equation 7, the effects of with spanwisely varying chord and flap geometries are included to the problem.

Aerodynamic Formulation

The nonconservative generalized forces which come as a result of the aerodynamic environment are presented in this section. In present formulation, the aerodynamic terms are determined by from Greenberg's extension of Theodorsen's theory as presented in reference [10] for thin, two-dimensional airfoils undergoing unsteady motion in a time-varying incompressible free-stream. As formulated in reference [9] Theodorsen theory faciliates chordwise rigid airfoil with aerodynamically unbalanced trailling edge flap or control surface hinged at $x = bc_f$. The airfoil may have move in vertical translation $h(t)$ and rotate about an axis at $x = ba$ through an angle $\alpha(t)$ and $\Lambda(t)$ represents the angular displacement of the flap relative to the chordline of the airfoil. The positive direction of these variables are as illustrated in Figure 2.

A quasi-steady aerodynamic approximation is employed wherein Theodorsen's lift deficiency function $C(k)$ is taken as equal to unity. The circulatory and noncirculatory lift and moment per unit span, assuming pitch occurs about the quarter chord can be written based on the the derivation given in reference [9] where circulatory and noncirculatory lift components are derived as;

$$L_C = \frac{1}{2}\rho a c U\left[-U_P + \frac{c}{2}\dot{\alpha}\right] + \rho c U\left[U\Lambda f_1 + \frac{c}{4}\dot{\Lambda} f_2\right] \tag{8}$$

$$L_{NC} = \frac{1}{2}\rho a \frac{c^2}{4}\left[-\dot{U}_P + \frac{c}{4}\ddot{\alpha}\right] - \rho\frac{c^2}{4}\left[U\dot{\Lambda}f_3 + \frac{c}{2}\ddot{\Lambda}f_4\right] \tag{9}$$

and the sectional aerodynamic pitching moment is expressed as,

$$M_\phi = \frac{1}{2}\rho a\left\{\frac{c^3}{16}\left[\dot{U}_P - U\dot{\alpha} - \frac{3c}{8}\ddot{\alpha}\right] - \frac{1}{2}\frac{c^3}{4\pi}\left[U\dot{\Lambda}(\frac{f_2}{2} + f_7) + \frac{c}{2}\ddot{\Lambda}f_8\right] + \frac{c^2}{4\pi}\left[-U^2\Lambda(f_1 + f_3)\right]\right\} \tag{10}$$

Specifically for the rotary wing aerodynamic representation, U_P is related to $\dot{h}$ and $U\alpha$ in reference [12] as

$$U_P \approx= -(\dot{h} + U\alpha)$$

The total velocity, U is the resultant of vertical and tangential velocities as

$$U^2 = U_T^2 + U_P^2$$

U_T and U_P are given in nondimentional form in reference [11] in terms of the elastic varibles, spanwise and azimuthal location, pitch, inflow ratio, rotor rotational velocity and advance ratio as,

$$U_T = \overset{*}{v} + (x + \mu\sin\psi) + \mu v^+\cos\psi \tag{11}$$

$$\begin{aligned} U_P &= \overset{*}{w} - \mu(\theta+\phi)v^+\cos\psi + \mu(w^+ + \beta_{pc})\cos\psi - \lambda + (w^+v + v\beta_{pc}) - \overset{*}{v}(\theta+\phi) \\ &- (\theta + \phi + v^+w^+)(x + \mu\sin\psi) \end{aligned} \tag{12}$$

Finally the lift components in lead-lag and flap directions are expressed in terms of the circulatory and noncirculatory lift components in reference [10] as

$$L_v = -(\theta+\phi)(L_C\cos\varrho + L_{NC} - D\sin\varrho) + (-L_C\sin\varrho - D\cos\varrho) \tag{13}$$

$$L_w = (L_C\cos\varrho + L_{NC} - D\sin\varrho) - (\theta+\phi)(L_C\sin\varrho + D\cos\varrho) \tag{14}$$

where the airfoil sectional drag is approximated as

$$D = \frac{1}{2}\rho c C_{D0}U^2$$

with the geometric relations illustrated in Figure 2,

$$\sin\varrho = \frac{U_P}{U}, \quad \cos\varrho = \frac{U_T}{U}$$

the lift components are writeen in nondimensional form as

$$\begin{aligned} L_v &= \frac{\gamma}{6}\left\{\left[U_P^2 - \frac{c}{2}U_P\overset{*}{\alpha}\right] + \frac{C_{D0}}{a}\left[U_TU_P(\theta+\phi) - U_T^2\right]\right. \\ &+ (\theta+\phi)\left[U_TU_P - \frac{c}{2}U_T\overset{*}{\alpha} + \frac{c}{4}\overset{*}{U_P}\right] - \frac{2}{a}\left[U_PU_T\Lambda f_1 + \frac{c}{4}U_P\overset{*}{\Lambda}f_2\right] \\ &- \left.\frac{2}{a}(\theta+\phi)\left[U_T^2\Lambda f_1 + \frac{c}{4}U_T\overset{*}{\Lambda}f_2\right] + (\theta+\phi)\frac{c}{2a}\left[U_T\overset{*}{\Lambda}f_3 + \frac{c}{2}\overset{**}{\Lambda}f_4\right]\right\} \end{aligned} \tag{15}$$

$$\begin{aligned} L_w &= \frac{\gamma}{6}\left\{\left[-U_PU_T + \frac{c}{2}U_T\overset{*}{\alpha} - \frac{c}{4}\overset{*}{U_P}\right] - (\theta+\phi)\left[-U_P^2 + \frac{c}{2}U_P\overset{*}{\alpha} + \frac{C_{D0}}{a}U_T^2\right]\right. \\ &+ \frac{2}{a}\left[U_T^2\Lambda f_1 + \frac{c}{4}U_T\overset{*}{\Lambda}f_2\right] - \frac{C_{D0}}{a}U_TU_P - \frac{2}{a}(\theta+\phi)\left[U_TU_P\Lambda f_1 + \frac{c}{4}U_P\overset{*}{\Lambda}f_2\right] \\ &- \left.\frac{c}{2a}\left[U_T\overset{*}{\Lambda}f_3 + \frac{c}{2}\overset{**}{\Lambda}f_4\right]\right\} \end{aligned} \tag{16}$$

$$M_\phi = \frac{\gamma}{6}\frac{c}{4}\left\{\frac{c}{4}\left[\overset{*}{U_P} - U_T\overset{*}{\alpha} - \frac{3c}{8}\overset{**}{\alpha}\right] - \frac{1}{a}\left[2U_T^2\Lambda(f_1+f_3) + \frac{c^2}{2}\overset{**}{\Lambda}f_8 + c\,U_T\overset{*}{\Lambda}\left(\frac{f_2}{2} + f_7\right)\right]\right\} \tag{17}$$

SOLUTION METHOD

Rotor Blade Nonlinear Partial Differential Equations

Several methods have been developed for the solution of nonlinear coupled partial differential equations representing the flap-lag-torsion motions of hingeless and bearingless rotor blades. A conditionally stable, explicit finite difference scheme to numerically integrate the nonlinear partial differential equations in space and time to obtain the aeroelastic response of elastic rotor blades has been introduced in references [13, 14]. An identical numerical formulation is also used in reference [5] to obtain the steady-state response of elastic hingeless rotor blades with flap control inputs and the numerical scheme is adopted to calculate various transient responses with this study. For purposes of numerical integration by the proposed approach which is based on explicit finite difference methods, it is convenient to express the coupled nonlinear partial differential equations of rotor blade system in terms of first order time and second order space derivatives. This reduction is performed by introducing the following variables.

$$v_t = \overset{*}{\bar{v}}, \quad w_t = \overset{*}{\bar{w}}, \quad \phi_t = \overset{*}{\bar{\phi}} \tag{18}$$

and

$$m_v = \bar{v}^{++}, \quad m_w = \bar{w}^{++} \tag{19}$$

similary,

$$\overset{*}{m_v} = v_t^{++}, \quad \overset{*}{m_w} = w_t^{++} \tag{20}$$

where $()^*$ and $()^+$ are the partial derivatives with respect to nondimensional time variable, ψ, azimuth angle, and nondimensional spanwise location variable, $\bar{x}$, respectively. In terms of these variables, rotor blade nonlinear, coupled partial differential equations and the trailing terms given in reference [10] are reorganized in reference [13] matrix form as follows,

$$\begin{aligned}
\overset{*}{\mathbf{u}_t} &= \bar{\mathbf{A}}(\mathbf{u},\psi)\mathbf{u}_m^{++} + \bar{\mathbf{B}}(\mathbf{u},\psi)\mathbf{u}_d^{++} \\
&\quad + \bar{\mathbf{C}}(\mathbf{u},\psi)\mathbf{u}_d^{+} + \bar{\mathbf{D}}\mathbf{u}_t \\
&\quad + \bar{\mathbf{E}}(\mathbf{u},\psi)\mathbf{u}_m + \bar{\mathbf{F}}(\psi)\mathbf{u}_d + \bar{\mathbf{g}}(\mathbf{u},\psi) \\
\overset{*}{\mathbf{u}_m} &= \mathbf{I}_{23}\mathbf{u}_t^{++} \\
\overset{*}{\mathbf{u}_d} &= \mathbf{I}_{33}\mathbf{u}_t
\end{aligned} \tag{21}$$

where $\mathbf{u}_d$ and $\mathbf{u}_t$ are displacement and velocity vectors respectively. The quantity $\mathbf{u}_m$ is vector defined in the following set of equations.

$$\mathbf{u}_t = \{v_t, w_t, \phi_t\}^T, \mathbf{u}_m = \{m_v, m_w\}^T \mathbf{u}_d = \left\{\bar{v}, \bar{w}, \bar{\phi}\right\}^T \tag{22}$$

Details of the formulation are given in refrences [13, 14]

The Explicit Time Finite Difference Method

Finite difference approximations for rotor blade equations can be formulated in different ways. For time derivatives $\mathbf{u}_{t_i}^{j+1}$, the exact solutions of the rotor blade partial differential equations 21 the node point $(\bar{x}_i, \psi_j + \Delta\psi)$ can be expanded in Taylor series as

$$\mathbf{u}_{t_i}^{j+1} = \mathbf{u}_{t_i}^{j} + \Delta\psi\mathbf{u}_{t_i}^{j^*} + \frac{1}{2}\Delta\psi^2\mathbf{u}_{t_i}^{j^{**}} + O(\Delta\psi^3) \tag{23}$$

Vectors $\mathbf{q}_{t_i}^j, \mathbf{q}_{m_i}^j$ and $\mathbf{q}_{d_i}^j$ are defined as approximations for $\mathbf{u}_t, \mathbf{u}_m$ and $\mathbf{u}_d$ at mesh point $(\bar{x}_i, \psi_{j+1})$ when only terms of the order of $\delta\psi$ are retained. Then, they can be combined into a vector $\mathbf{q}_i^j$ as

$$\mathbf{q}_i^j = \left\{\mathbf{q}_{t_i}^j, \quad \mathbf{q}_{m_i}^j, \quad \mathbf{q}_{d_i}^j\right\}^T$$

With these approximations for time derivatives, a conditionally stable, explicit scheme can be introduced by using different azimuthal level substitution into equation 21. This scheme can be

written as, at $(i, j+1)^{th}$ mesh position in a matrix form as

$$\begin{aligned}
\mathbf{q}_{t_i}^{j+1} &= \mathbf{q}_{t_i}^{j} + \Delta\psi \left\{ \bar{\mathbf{A}}_i^j \delta^2 \mathbf{q}_{m_i}^j + \bar{\mathbf{B}}_i^j \delta^2 \mathbf{q}_{d_i}^j \right. \\
&\quad + \bar{\mathbf{C}}_i^j \delta \mathbf{q}_{d_i}^j + \bar{\mathbf{D}}_i^j \mathbf{q}_{t_i}^j + \bar{\mathbf{E}}_i^j \mathbf{q}_{m_i}^j \\
&\quad \left. + \bar{\mathbf{F}}_i^j \mathbf{q}_{d_i}^j + \bar{\mathbf{g}}_i^j \right\} + O(\Delta\psi^2) \\
\mathbf{q}_{m_i}^{j+1} &= \mathbf{q}_{m_i}^{j} + \Delta\psi \mathbf{I}_{23} \delta^2 \mathbf{q}_{t_i}^{j+1} + O(\Delta\psi^2) \\
\mathbf{q}_{d_i}^{j+1} &= \mathbf{q}_{d_i}^{j} + \Delta\psi \mathbf{I}_{33} \mathbf{q}_{t_i}^{j+1} + O(\Delta\psi^2)
\end{aligned} \tag{24}$$

In equation 24, δ and δ^2 are first and second order approximations tor first and second spatial derivatives respectively. In order to obtain a finite difference approximations to spatial derivatives the region to be examined is covered by a rectilinear grid with sides parallel to the x-axis and ψ-axis, with $\Delta\psi$ being the grid spacing in the ψ direction. The x-axis is divided into equal grids with lines paralell to the ψ-axis with coordiates $x = x_i, i = 0, 2, \ldots, m$ where $x_0 = 0$ and $x_n = 1$. This forms a grid rectangular time finite elements in time and space. The mesh points (x, ψ) are given by $x = x_i$, $\psi = N\Delta\psi$, where N is number of time intervals and $x_0 = 0$, $m = 0$ is the origin.

The currently calculated velocity vectors $\mathbf{q}_{t_i}^{j+1}$ are substituted into equation 24 to calculate defined variables $\mathbf{q}_{m_i}^{j+1}$. As explained later, this procedure makes the overall solution of the set of finite difference equations stable. The equation 24 depend on velocity vector $\mathbf{q}_{d_i}^{j+1}$ and it has been observed that averaging the velocitites vector $\mathbf{q}_{t_i}^{j+1}$ and $\mathbf{q}_{t_i}^{j}$ to calculate displacements has a destabilizing effect on the general solution of the numerical scheme. Therefore, displacements are calculated without averaging the velocities. Second order accuracy is obtained for spatial derivatives by central differencing. The accuracy of displacements, velocities and are defined variables are still first order in time. Details of the above described numerical scheme is given in refences [13] and [14].

RESULTS AND DISCUSSIONS

In this section numerical results are presented to illustrate the application of the approximate method to solve rotor blade aeroelastic equations. Since the objective of this paper is primarily to illustrate the application of the approximate method to find transient and steady-state response of rotor blades with cyclic flap controls in forward flight conditions, certain simplifications and assumptions are made as follows.

- For forward flight condition, inflow is assumed to be uniform along the blade and cyclic inflow components are set equal to zero. Uniform inflow λ_0 is written as

$$\lambda_0 = \mu \tan\alpha_v + \frac{C_T}{2(\mu^2 + \lambda_0^2)^{\frac{1}{2}}} \tag{25}$$

- Hub and tip loses are not included.
- A two dimensional, strip type, quasiateady aerodynamic model is used where Theodorsen lift deficiency function $C(k)$ is set equal to unity.
- Structural and mass properties of the blade are assumed to be uniform along the blade. All offsets from the elastic axis are also neglected.
- Reverse flow effects are not included.

Solutions for forward flight are initiated by setting all elastic deformation to zero and cyclic control components to the corresponding control input variation by a linear incremental procedure until their trim solutions values are reached. Increment for a control variable C_v is introduced as,

$$C_v^{j+1} = C_v^j + \Delta C_v$$

where

$$\Delta C_v = \frac{C_v}{N_{sw}}$$

Then the cyclic variation at $(j+1)^{th}$ azimuth step during this switching period is calculated as

$$C^{j+1} = C_0^{j+1} + C_{1S}^{j+1} \sin\psi_{j+1} + C_{1C}^{j+1} \cos\psi_{j+1}$$

In above expression C_0, C_{1C} and C_{1S} are the control inputs obtained by trim solution and N_{sw} is the number of the azimuthal steps of this switching period.

Results are obtained flap controlled rotor blade stopping conditions. Basic rotor and vehicle parameters of the considered 700 lb micro-helicopter configuration are given in Table 1. Maximum rotor angular speed is taken as $\Omega = 80$ rad/sec for this configuration.

Parameters related with the choosen configuration are obtained by a simplified preliminary design approach as being necessary inputs for the present analysis. The considered rotor blade has a rectengular planeform with chord width c= 1.0 ft., and uniform flap along the rotor span with nondimensional flap hinge offset from center chord, c_f= 0.4. Rotor blade pre-wist θ_{tw} taken as -0.08 rad. and a rigid pitch setting is taken as, θ_{ri}= 0.10 rad.

Approximate trim solutions are coupled with the nonlinear rotor blade P.D.E. solver to simulate blade dynamics. Transient response calculations are started for initial hover condition by simply setting advance ratio $\mu = 0.0$ and forward flight speed is gradually increased by intervals of $\Delta\mu = .025$. Variation of advance ratio respect to rotor angular speed change is shown in Figure 3. Flap control inputs variation is also illustrated in Figure 4 and as seen from figure higher flap control components are required for slowing rotor contition where rotor speed is reduced from $\omega = 80$ to $\omega = 40$ rad/sec as blades still generating some trust to partially lift the vehicle.

Rotor Stop Formulation

For the rotor speed reduction period and the related deficiency in the rotor thrust lift component, the helicopter is utilized by additional lifting device such as two canards located in front of the vehicle c.g. as shown in with the general helicopter configuration, Figure 1. The helicopter has speed V and a flight path angle θ_{fp}, so that a climb or descent velocity $V_c = V \sin\theta_{fp}$ is considered. The reference plane has angle of attack α with respect to the forward speed. The forces active on the vehicle are the weight W (vertical), aerodynamic drag D, rotor thrust T_{MR}, rotor trust component H and canard lift L_{can}. Vertical and horizontal force equilibrium,

$$W = T_{MR}\cos(\alpha - \theta_{FP}) - D\sin\theta_{FP} + H\sin(\alpha - \theta_{FP}) + L_{CAN}\cos\theta_{FP} \tag{26}$$

$$T_{MR}\sin(\alpha - \theta_{FP}) - L_{CAN}\sin\theta_{FP} = D\cos\theta_{FP} + H\cos(\alpha - \theta_{FP}) \tag{27}$$

For a given forward speed V, rotor angular speed ω, flight path angle θ_{FP}, vehicle angle of attack α and the given engine Q_{MR}, the rotor thrust T_{MR} and the required canard lift L_{CAN}, to maintain the helicopter in the desired forward flight conditions are calculated by the use of equations 26 and 27 respectively.

The flap control variation during this two stage transition; vehicle forward speed increase and rotor slow down are shown in Figure 5. Since the mean trust is obtained by the rigid pitch, the collective flap input Λ_0 is reduced as advance ratio μ is varied from 0 to 0.25. All flap control inputs are increased as the blade rpm decreased (as relative velocity acting to the blade is decreased). Physically chamber of the blade cross section is needed to be increased to generate lift as the acting air velocity decreased.

Blade elastic tip deflections in edgewise (inplane) and flapwise directions are illustrated in Figures 6 and 7 respectively. The transient lead-lag tip deflections are observed to be in same characteristics during vehicle forward flight acceleration. As also expected initially, blade elastic response is increased during rotor blade slowing down and rotor instability is observed before rotor reached its desired final rpm. Flapping tip deflections found to be more stable as seen from Figure 6 for the choosen blade parameters.

CONCLUSIONS AND REMARKS

Since the major objective of this study was to develop a numerical tool to simulate elastic blade response for rotor transition modes, a specific emphasis was not given for the search and design of an particular blade or helicopter configuration. A systematic study must be done for a clear understanding of the blade transition dynamics and for the proper selection of blade stiffness and mass properties for a stable stopped/flipped rotor configuration. The approximate trim formulation found to be efficient for initial performance calculations and trim solutins obtained for torsionally stiff configurations can be within the accuracy of conventional pitch control trim calculations.

The aerodynamic formulation for the unsteady oscillating rotor blade airfoil with trailing edge flap controls and conditionally stable explicit finite difference scheme is found to be an effective method for response simulations. With the use of paralel computing hardware and software capabilities of today's computer technologies it is also believed it can be also efficient tool for the simulation of rotorcraft configurations with flap controls.

Based on this initial study, existing study need to be extended to below described areas;

Number of blades	$b = 2$	Main rotor radius	$R_{MR} = 8$ ft
Main rotor speed	$\Omega_{MR} = 80$ rad/sec	Ave. main chord	$c_{MR} = 1$ ft
Ave. flap width ratio	$c_f = 0.4$	Offsets from c.g.	$x_{cg} = 0.125$ ft h_t=1.8 ft
Gross weight	$W_g = 700$ lb	First lag frequency :	Λ_2=.04
First flap frequency :	Λ_1 =.0306	First torsion frequency :	$\bar{G}J$=.0625
Cross sectional inertias	$\left(\frac{k_A}{k_M}\right)^2 = 1.0$	$\left(\frac{k_M}{R}\right) = .025$	$\left(\frac{k_{m_1}}{k_{m_2}}\right) = 0.0$
Semicord :	$\frac{b}{R}$, variable	Drag coefficient :	C_{D0}=0.01
Solidity ratio :	σ=0.08	Lock number :	γ=6.
2-D Lift curve slope :	$a = 2\pi$	Aerodynamic center offset	X_A=0.0
Precone angle	β_p=0.0	Advance ratio	μ, variable
Blade rigid pitch	$\theta_{ri} = 0.10$ rad	Blade pretwist angle	θ_{tw} = -.08 rad

Table 1: Stop Rotor Blade and Vehicle Configuration Parameters for Flap-Lag-Torsion Motions in Forward Flight

- Composite rotor blade formulations representing the bending-torsion couplings must be included to the problem therefore composite blade-highly elastic flap congirations combinations can be investigated.
- Elastic trim formulations are needed to be included to the problem for a better formulation and the simulation of the lift variations due to the elastic twist of the blade.
- Higher harmonics of the flap control inputs are needed to be included both in trim formulations and elastic response calculations to simulate and analyze flap controlled blades with High Harmonic Control and Individual Blade Control applications.

Acknowledgement

Authors greatly acknowledge Prof. D.P. Shrage and Asst. Prof. J.V.R. Prasad at CERWAT and School of Aerospace Engineering, Georgia Institute of Technology, USA for their comments and stimulating discussions. Authors also wish to thank Mr. E. Kisli, Project Engineer at Undersecretariat For Defense Industries, Turkiye for his support in computations.

References

[1] Lemnios, A.Z.; and Jones, R.: "The Servo Flap- An Advanced Rotor Control System", Presented at the AHS Design Specialist Meeting on Vertical Lift Aircraft Design, San Francisco, California, 17-19 January 1990.

[2] Phillips, N.B.; and Merkley, D.J.: " BHTI's Technical Assessment of Advanced Rotor and Control Concepts", Presented at the AHS Design Specialists' Meeting on Vertical Lift Aircraft Design, San Francisco, California, 17-19 January 1990.

[3] Straub, F.K.; and Merkley, D.J.: " MDHC's Technical Assessment of Advanced Rotor and Control Concepts", Presented at the AHS Design Specialists' Meeting on Vertical Lift Aircraft Design, San Francisco, California, 17-19 January 1990.

[4] Yillikci, Y.K.: "Triming Rotor Blades with Periodically Deflecting Trailing Edge Flaps", Presented at the 17th European Rotorcraft Forum", September 24-26, 1991, Berlin, Germany.

[5] Yillikci, Y.K.; Hanagud, S.V.; Schrage, D.P.; Higman, J.: " Aeroelastic Analysis of Rotor Blades With Flap Control", Presented at the 18th European Rotorcraft Forum, September 15-18 1992, Avignon, France.

[6] Blanchette, B.M.: "Design and Construction of A ShipLaunched VTOL Unmanned Air Vehicle, Thesis, Naval Postgraduate School, Monterey CA, June 1990.

[7] Kisli, E.; Prasad, J.V.; Yillikci, Y.K.: "Conceptual Design of A Stopped Rotor With Flap Controls", Presented at the 18th European Rotorcraft Forum, September 15-18 1992, Avignon, France.

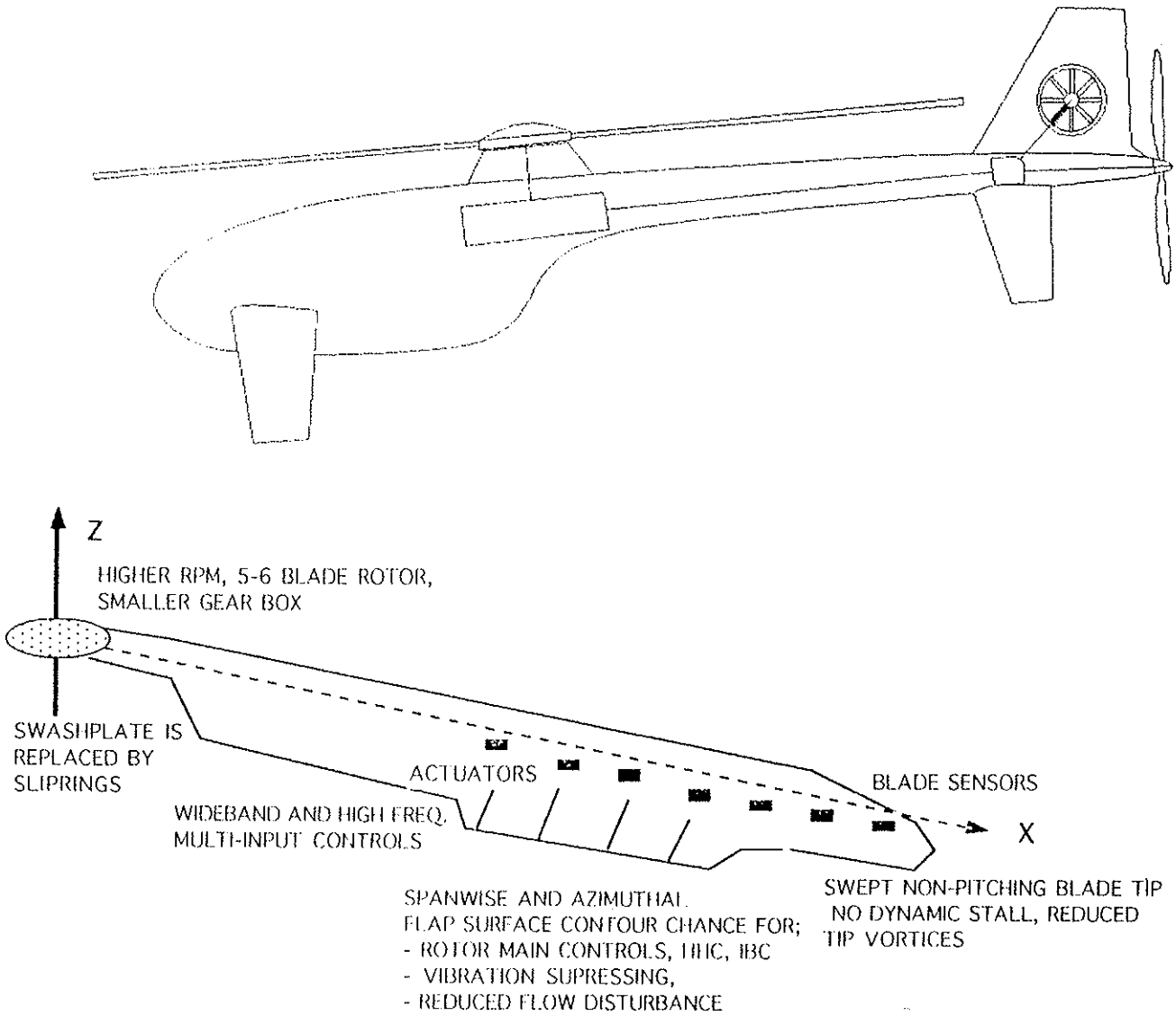

Figure 1: General Concept of Flap Controlled Rotor Blades and Stopped/Flipped Rotor

[8] Johnson, W.: *Helicopter Theory*, ch.2 Princeton, 1980.

[9] "Bishlinghoff, R.L.; Asley, H; Halfman, R.L.: *Aeroelasticity*, Addison Wesley Publishing Company, 1975.

[10] Taylor, D. J., "A Method for the Efficient Calculation of Elastic Rotor Blade Dynamic Response in Forward Flight ", Doctoral Dissertation, School of Aerospace Engineering, Georgia Institute of Technology, Atlanta, Georgia, March 1987.

[11] Pierce, G.A.; and Hamouda, M.H.: "Helicopter Vibration Supression Using Pendulum Absorbers on the Rotor Blade", NASA CR 3619, 1982.

[12] Kaza, K.R.V.; and Kvaternik, R.G.: "Engineering Notes- Application of Unsteady Airfoil Theory to Rotary Wings", Journal of Aircraft, Vol. 18, No. 7, 1981

[13] Yillikci, Y.K.:"Finite Difference Techniques and Rotor Blade Aeroelastic Partial Differential Equations with Quasisteady Aerodynamics", Doctoral Dissertation, School of Aerospace Engineering, Georgia Institute of Technology , Atlanta, Georgia, December, 1988.

[14] Yillikci, Y.K.; and Hanagud, S.: "Finite Difference Techniques and Rotor Blade Aeroelastic Partial Differential Equations: An Explicit Time-Space Finite Element Approach For P.D.E.", Presented at the 15th European Rotorcraft Forum, September 12-15, 1989, Amsterdam, Netherlands.Technology , Atlanta, Georgia, December, 1988.

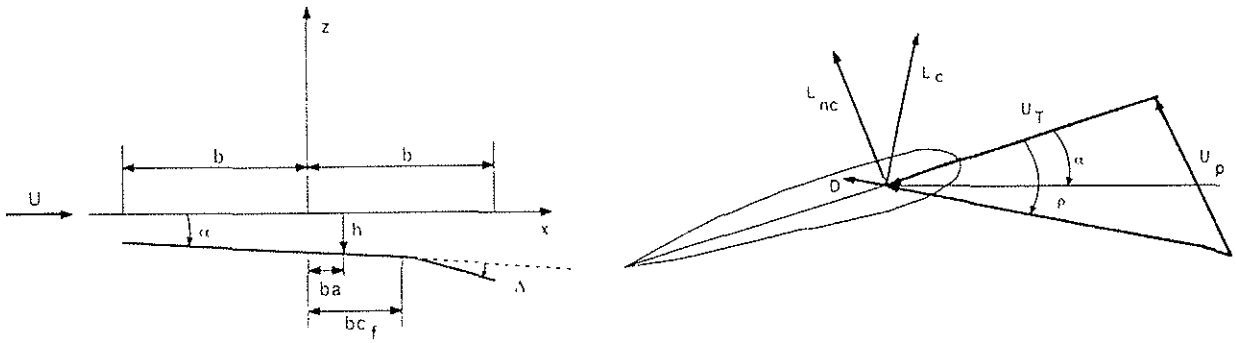

Figure 2: 2-D Oscillating Airfoil Description, Aerodynamic Force and Velocity Components.

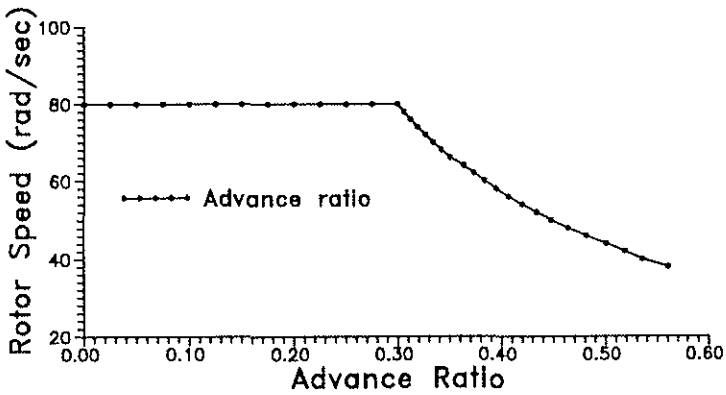

Figure 3: Advance Ratio Variation During Rotor Rpm Changes.

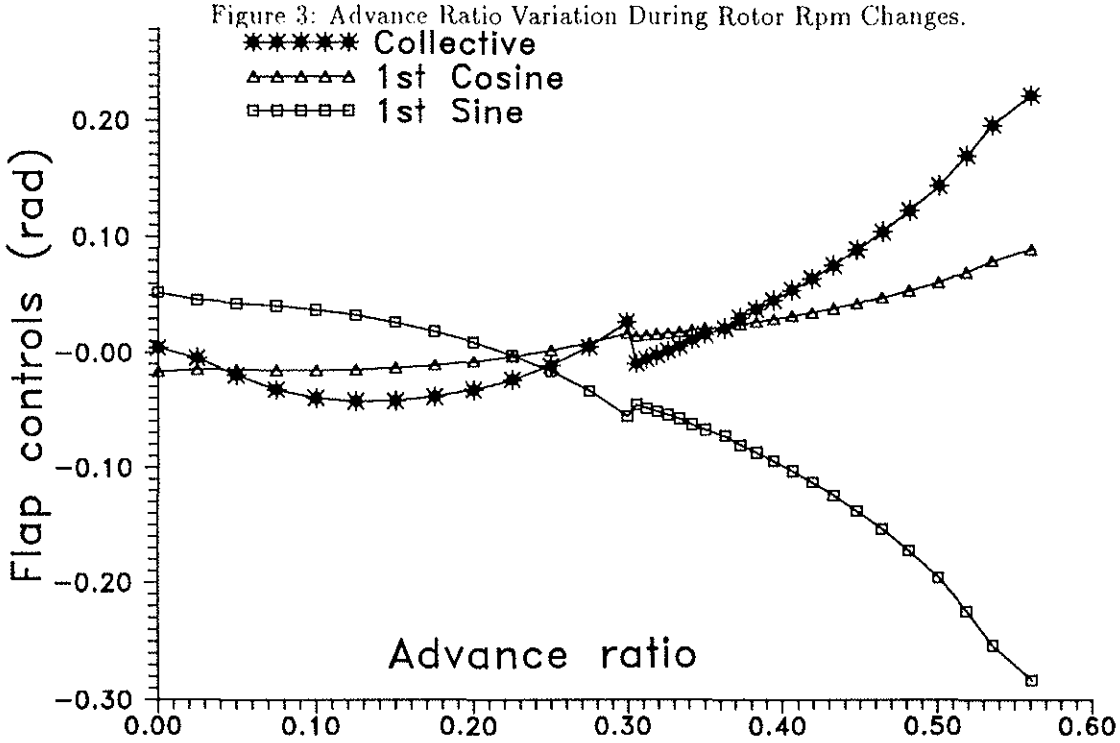

Figure 4: Flap Control Inputs for Forward Flight and Rotor Stopping Modes.

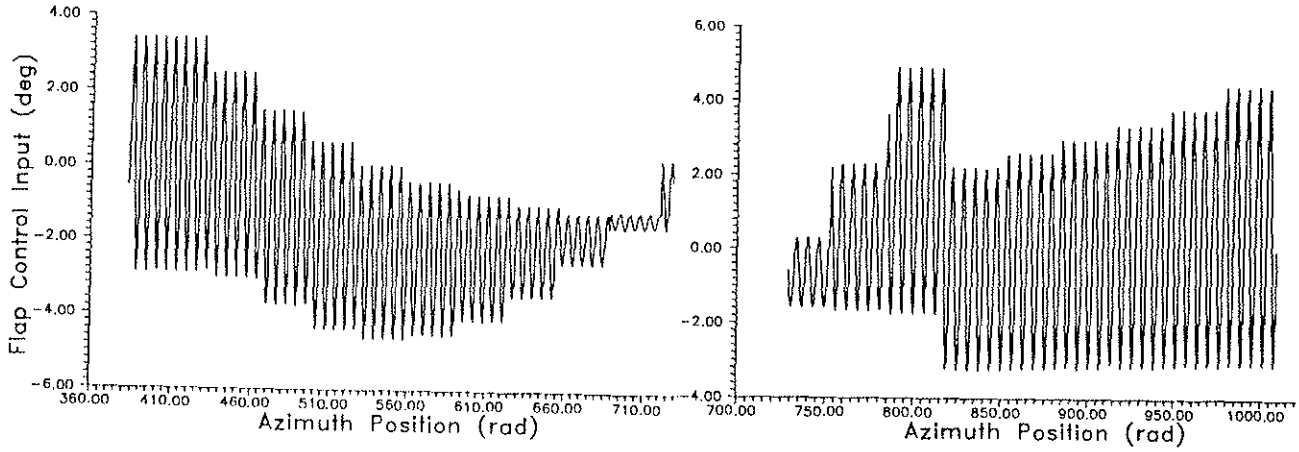

Figure 5: Flap Controls Variation During Forward Flight and Rotor Stop.

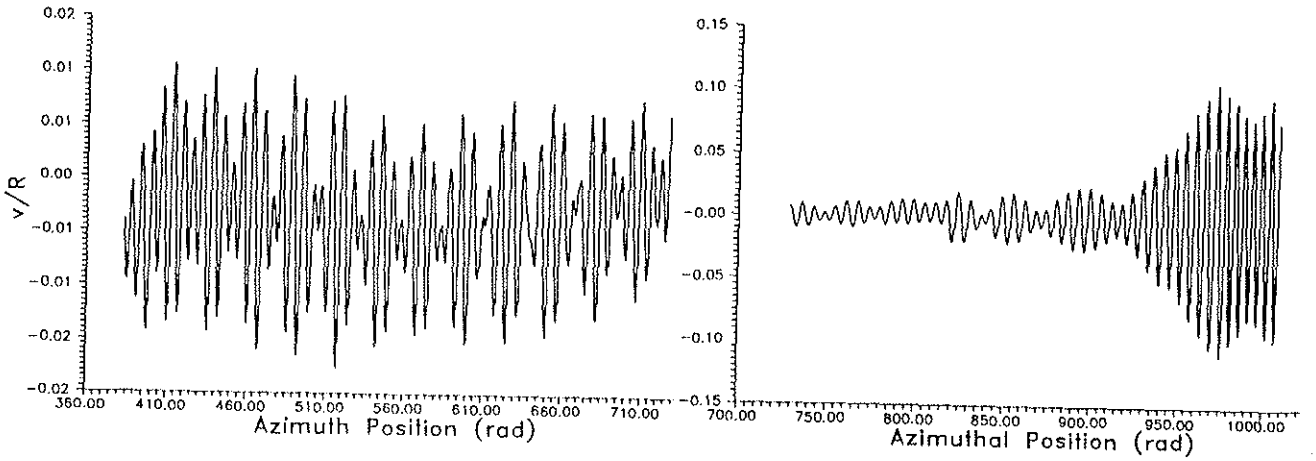

Figure 6: Transient Elastic Inplane Tip Response During Forward Flight and Rotor Stop.

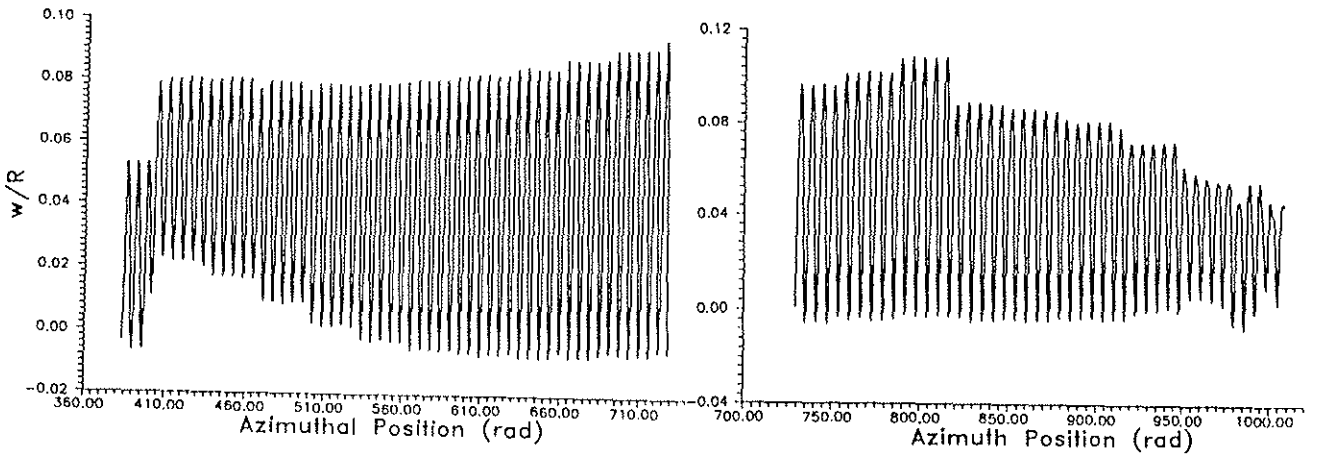

Figure 7: Transient Elastic Flapping Tip Response During Forward Flight and Rotor Stop.